RECENT PHYSICS RESULTS FROM THE D0 EXPERIMENT

PNPI participants of the D0 Collaboration:
G.D. Alkhazov, V.T. Kim, A.A. Lobodenko, P.V. Neustroev, G.Z. Obrant, Yu.A. Scheglov, L.N. Uvarov, S.L. Uvarov

1. Introduction

D0 is an international collaboration of about 670 physicists from 83 institutions, who have designed, built and are operating a collider detector at the Fermilab Tevatron.

Main physics goals are precision tests of the Standard Model (SM), the weak bosons physics, top quark physics, QCD, *B* physics and a search for particles and forces beyond the SM: super-symmetric (SUSY) particles, gravitons, candidates for the cosmic dark matter, and a search for extra dimensions.

During Run II, the Tevatron is operated at an increased $p\bar{p}$ center-of-mass energy of 1.96 TeV. The luminosity has been increased by a factor more than ten, to $\geq 10^{32}$ $cm^{-2}\,s^{-1}$.

PNPI has been involved in the D0 project through the design and programming of the electronic readout for mini drift tubes (50,000 channels) and operation of the Forward Muon System [1]. PNPI physicists take part in the data analysis, including QCD, *B* physics, and Electroweak physics studies. Main D0 physics results are the top-quark mass, B_s mixing frequency, cross section for single top-quark production and inclusive cross section.

2. The D0 detector

The Run II D0 detector (Fig. 1) [2] consists of a central tracking system, a liquid-argon/uranium sampling calorimeter and an iron toroid muon spectrometer.

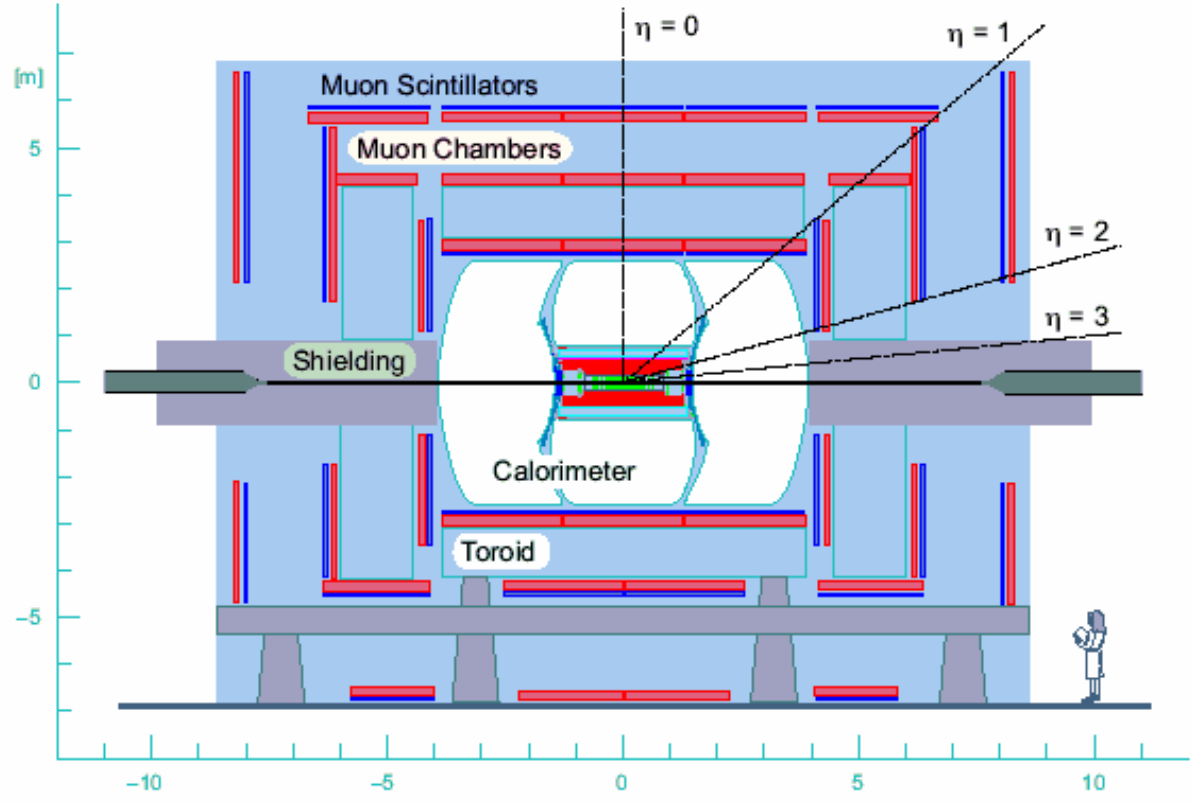

Fig. 1. A schematic view of the D0 detector

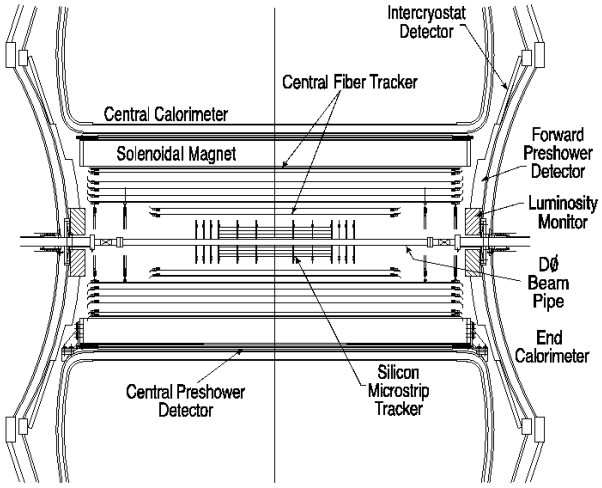

Fig. 2. Cross-sectional view of the new central tracking system in the XZ plane

The central tracking system (Fig. 2) is composed of a silicon microstrip tracker (SMT) and a central fiber tracker, both located into a 2T superconducting solenoidal magnet. The SMT detector has about 800,000 individual strips, and its design is optimized for tracking and vertexing capabilities allowing heavy flavor tagging. The calorimeter is longitudinally segmented into electromagnetic and hadronic layers and is housed into three cryostats. The muon system [3] resides beyond the calorimeter and consists of a layer of tracking detectors and scintillation counters before the toroidal magnet, followed by two similar layers after the toroid. Tracking in the muon system relies on wide or mini drift tubes depending on the acceptance. The Run II D0 detector allows to work at the luminosity of $>10^{32}$ cm^{-2} s^{-1}. The D0 detector is described in detail in Ref. [2]. Most important recent physics results are presented below.

3. Top quark production cross section and mass

The t quark, the heaviest particle known, was discovered at the Tevatron in 1995. Since then, the study of the top quark was one of important directions of investigations at D0. In the triggering and analysis, the event selection was done with high p_T leptons, high E_T multiple jets, large missing energy E_T and displaced vertices for b-jets. The cross section for the $t\bar{t}$ production was measured by several methods. Two most precise results [4] for the $t\bar{t}$ production cross section are derived from the lepton + jets channel: $\sigma_{t\bar{t}} = 7.2 \pm 1.2 + 1.9 - 1.4$ pb, with an impact parameter tagging, and $\sigma_{t\bar{t}} = 8.2 \pm 1.3 + 1.9 - 1.8$ pb, using a vertex tagging.

Last measurements using the vertex tagging combines the μ + jets and e + jets channels, using 422 pb^{-1} and 425 pb^{-1} of data. The measured $t\bar{t}$ production cross section for a top-quark mass of 175 GeV is $\sigma_{t\bar{t}} = 6.6 \pm 0.9\,(\text{stat} + \text{syst}) \pm 0.4\,(\text{lum})$ pb.

The top-quark mass is a fundamental SM parameter. Together with the W mass, it provides a constraint on the Higgs mass. Different methods were used at D0 to derive the top-quark mass. The combined result for the top-quark mass, obtained by the D0 and CDF collaborations from the data of Run I and Run II, is [5]: $m_t = 172.5 \pm 2.3$ GeV/c^2 (Fig. 3). This is the most accurate measurement of the top-quark mass by now.

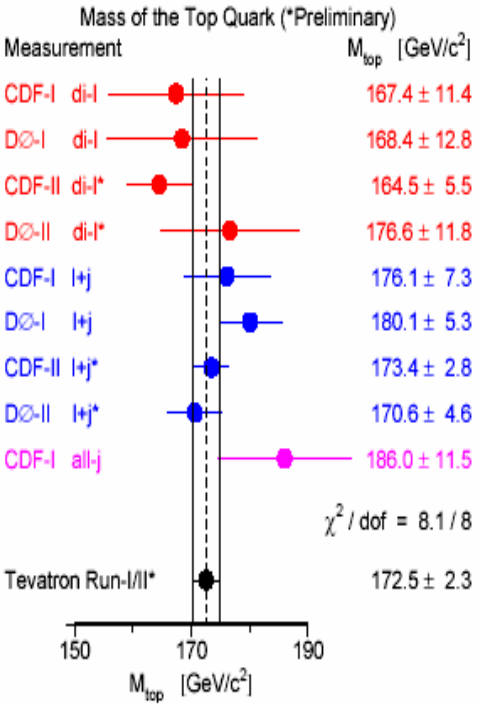

Fig. 3. Results of the t-quark mass measurements in the experiments D0 and CDF

4. Search for single top-quark production

For the first time, the top quark was observed in its $t\bar{t}$ production mode. The single top-quark production with the *tb* or *tqb* final states is possible *via* the electroweak interaction. A measurement of the single top-quark production cross section can be used to constrain the magnitude of the CKM matrix element V_{tb} and study the *Wtb* coupling. An events selection in the search for single top quarks is similar to the search for the top-quark pairs in the *l* + jets mode. Backgrounds of *W* + jets, $t\bar{t}$ and dibosons are substantial.

The D0 Collaboration presents a first evidence for the production of single top quarks at the Fermilab Tevatron $p\bar{p}$ collider. Using a 0.9 fb^{-1} data set and applying a multivariate analysis to separate signal from background, the cross section for the production of single top quarks in the reactions $p\bar{p} \rightarrow tb + X$, $p\bar{p} \rightarrow tqb + X$ was measured to be 4.9 ± 1.4 pb [6] (Fig. 4). The probability to measure a cross section at this value or higher in the absence of signal is 0.035%, corresponding to a 3.4 standard deviation significance. The measured cross section was used to directly determine the CKM matrix element that describes the *Wtb* coupling. The found value of V_{tb} is $0.68 < |V_{tb}| \leq 1$ at the 95% CL, which agrees with the SM.

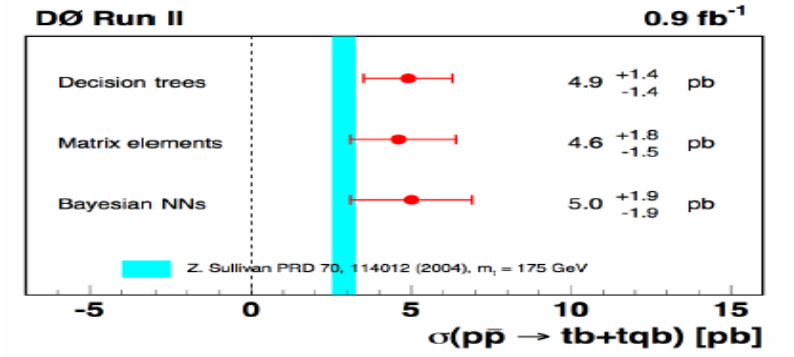

Fig. 4. Single top-quark production cross section, *s* + *t* channels

5. QCD studies

Motivations of the QCD studies are to use the strong interaction processes for an investigation of the internal proton structure, a search for the quark substructure, a study of the diffractive and heavy flavor production, a study of new objects, like *X*(3872), and for the understanding of backgrounds to the physics beyond the SM.

The D0 Run II results [7] cover the QCD cross section which changes up to 8 orders of magnitude. One of the most new QCD results is the inclusive photon cross section in the central rapidity region for p_T range of $23 < p_T$ [GeV/c] < 300 (Fig. 5). The dominant source of the photon production for $p_T < 150$ GeV/c is the prompt Compton quark-gluon scattering. The cross section for the inclusive photons is sensitive to the gluon parton distribution function. The gamma p_T values measured at D0 are much higher than those covered in previous experiments. The NLO QCD predictions describe the data within the experimental uncertainties in the whole p_T range considered.

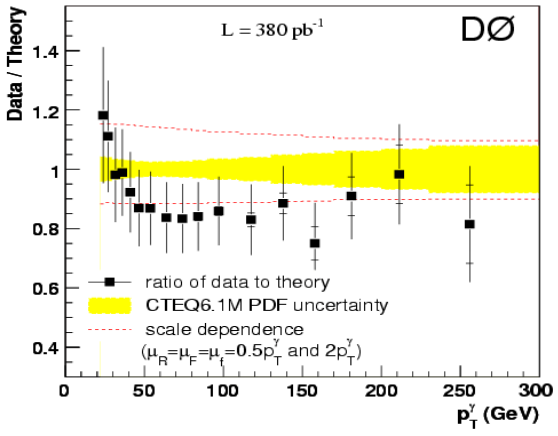

Fig. 5. Inclusive photon cross section in the central rapidity region: ratio of the experimental data to theory

6. Electroweak physics. Diboson production

One of the main motivations of the electroweak physics is to constrain indirectly new physics by means of precision measurements of electroweak parameters. The experimental cross sections for WW, WZ, ZZ, $W\gamma$ and $Z\gamma$ production provide a test of the SM and give information about boson self-coupling. Besides, the electroweak processes are backgrounds to many interesting searches, like $H \rightarrow WW$.

Measurements of a single and multi-boson production, a W production asymmetry, a forward-backward asymmetry in the Z-boson production and other electroweak processes are underway at D0 [8]. New experimental limits on Anomalous Couplings are set (Fig. 6) for $ZZ\gamma$ and $Z\gamma\gamma$: $|h_{30}^{\gamma}|<0.23$, $|h_{40}^{\gamma}|<0.019$, $|h_{30}^{Z}|<0.23$, $|h_{40}^{Z}|<0.20$ at the 95% CL for Λ=1 TeV, where Λ is a form factor scale displaying the scale of new physics. All cross sections are in good agreement with the SM.

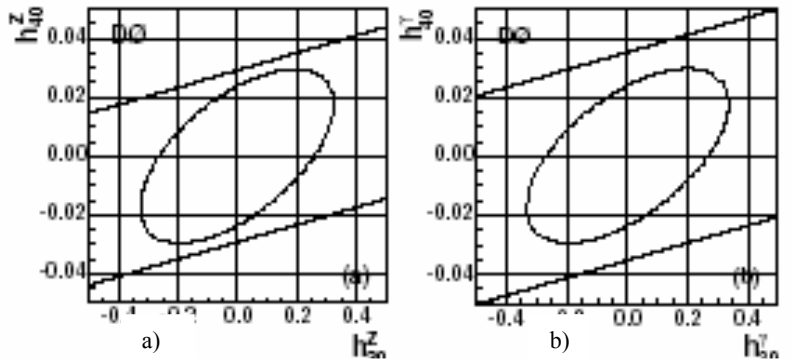

Fig. 6. The 95% CL two-dimensional exclusion limits for CP-conserving (a) $ZZ\gamma$ and (b) $Z\gamma\gamma$ couplings for Λ = 1 TeV. Straight lines illustrate the unitarity constraints

7. Search for the $B_s \rightarrow 2\mu$ decay

B physics is one of the important directions of studies at D0 [9]. A search for $B_s \rightarrow 2\mu$ of the flavor-changing neutral current decay helps to find an evidence of possible SM enhancements – the MSSM , SUSY, *etc*. The decay $B_s \rightarrow 2\mu$ is strongly suppressed in the SM. A contribution from all possible $B_s \rightarrow 2\mu$ SM diagrams gives the branching ratio ~3.5×10^{-9}. At the same time, in the MSSM this branching ratio can be up to 10^{-7}.

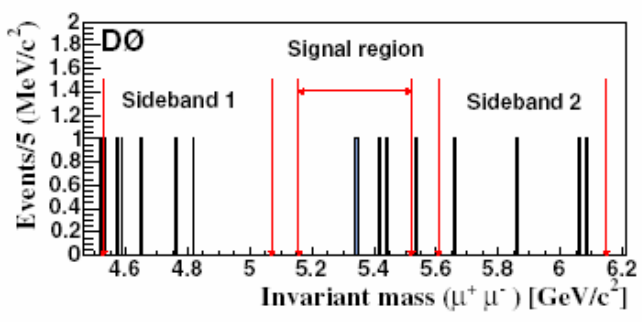

Fig. 7. Invariant mass of the remaining events of the full data sample after optimized requirements on discriminating variables

The silicon microstrip tracker allows to realize a search for the $B_s \rightarrow 2\mu$ rare decay. Since τ_{Bs} = 1.46 ps (400 μm), the secondary vertices of the B_s decay could be selected from the primary vertices. Figure 7 shows an invariant mass spectrum of $(\mu^{+}\mu^{-})$ events in the search region of the $B_s \rightarrow 2\mu$ decay. The D0 published an upper limit for this process: $BR\,(B_s \rightarrow 2\mu) < 5.0 \times 10^{-7}$ at the 95% CL [10]. A very recent new D0 preliminary result is: $BR\,(B_s \rightarrow 2\mu) < 1.1 \times 10^{-7}$ at the 95% CL.

The obtained results provide restrictions to many SUSY models. For example, last D0 and CDF results (the CDF result is $BR\,(B_s \rightarrow 2\mu) < 1.0 \times 10^{-7}$ at 95% CL) provide very strong restrictions to the parameters of the minimal supergravity scenario model mSUGRA and SO(10) SUSY symmetry breaking model.

8. B_s oscillations

One of the most interesting topics in B physics is the B_s^0 oscillations (or B_s^0 mixing – a transition of neutral B_s mesons between particle and antiparticle) and measurement of the oscillation frequencies Δm_s and Δm_d (correspondingly of B_s and B_d mesons). The values of Δm_s and Δm_d provide powerful constraints to the V_{td} and V_{ts} elements of the CKM matrix. The oscillation frequency Δm_d for B_d mesons was measured previously in the D0 and CDF experiments. As for B_s mesons, they are expected to oscillate much faster than B_d mesons. Consequently, their oscillations are more difficult to detect. Note that the ratio of the frequencies Δm_s and Δm_d is free of several theoretical uncertainties.

A search for the B_s^0 oscillations was performed at D0 using a semileptonic decay $B_s \to \mu D_s X$. D_s mesons were reconstructed *via* their decay channel $D_s \to \varphi\pi$, $\varphi \to KK$. As a result of this search, the D0 collaboration determined not only the lower boundary, but also the upper boundary of possible values of the B_s^0 oscillation frequency. The amplitude fit method of the data analysis gives a lower limit on the B_s^0 oscillation frequency at 14.8 ps^{-1} at the 95% CL. At Δm_s = 19 ps^{-1}, the amplitude deviates from the hypothesis of an oscillation amplitude of zero by 2.5 standard deviations (Fig. 8), corresponding to a two-sided CL of 1%. A likelihood scan over the oscillation frequency Δm_s gives a most probable value of 19 ps^{-1} and a range of $17 < \Delta m_s < 21$ ps^{-1} at the 90% CL [11]. This is the first direct two-sided bound on the B_s^0 oscillation frequency measured by a single experiment. The D0 result was confirmed shortly after by the CDF precise measurement: $\Delta m_s = 17.3 - 0.2 + 0.4 \pm 0.1$ ps^{-1}.

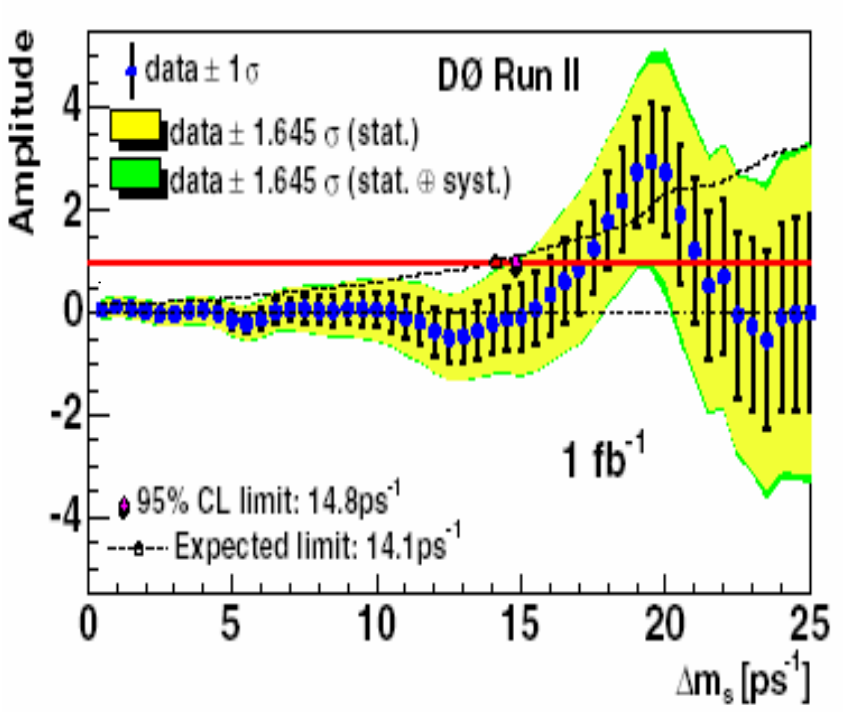

Fig. 8. B_s oscillation amplitude as a function of oscillation frequency Δm_s. The solid line shows the A = 1 axis for reference. The dashed line shows the expected limit including both statistical and systematic uncertainties

Systematic uncertainties of these measurements were addressed by varying inputs for a fitting procedure, cut requirements, branching ratios, and probability density function modeling. The branching ratios were varied within known uncertainties and large variations were taken for those not yet measured. The K-factor distributions were varied within uncertainties, using measured instead of generated momenta in the Monte Carlo simulation. The fractions of peaking and combinatorial backgrounds were varied within uncertainties. The lifetime of B_s^0 was fixed to its world average value, and $\Delta\Gamma_s$ was allowed to be nonzero. The scale factors on the signal and background resolutions were varied within uncertainties, and typically generated the largest systematic uncertainty.

9. Search for extra dimensions

A search for a virtual graviton exchange in Kaluza-Klein modes and Large Extra Dimensions in the channel of a real graviton emission is underway. A signal would be an excess of ee, $\mu\mu$ or $\gamma\gamma$ events at large invariant masses due to the virtual graviton exchange (Fig. 9). The latest D0 limit from the $p\bar{p} \to ee, \mu\mu$ and $\gamma\gamma$ events is MS (GRW) > 1.43 TeV at the 95% CL. This result is the most stringent limit to date on the Large Extra Dimensions [12].

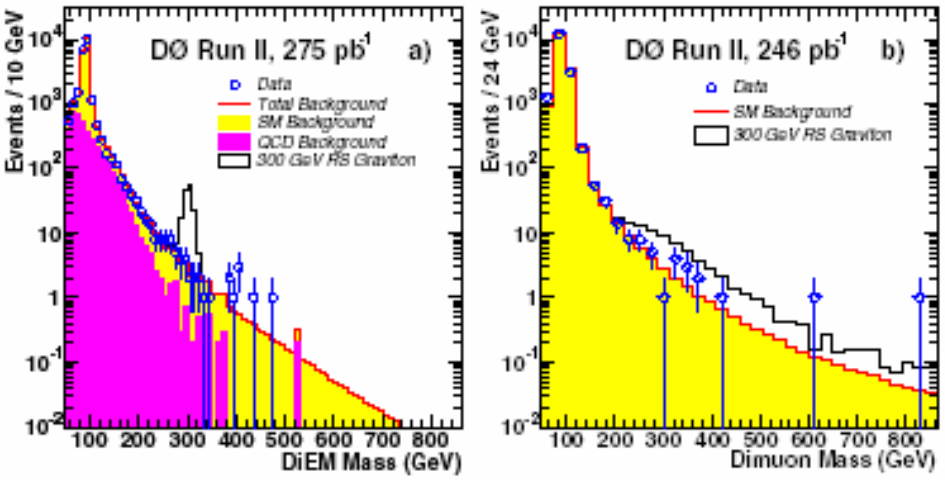

Fig. 9. Invariant mass spectrum in the (a) diEM and (b) dimuon channels. An open histogram is the signal from an RS graviton with the mass M_1 = 300 GeV and coupling k/M_{Pl}= 0.05

10. Search for SUSY particles

SUSY solves the "Hierarchy Problem" and provides the Grand Unification on the energy scale less than 10^{16} GeV. SUSY particles are good Dark Matter candidates. The D0 experiment realizes a search for the Chargino/Neutralino production in the $3l$ + missing E_T-channel and a search for Squarks and Gluinos (Fig. 10) in the channel jets + missing E_T. The Run II D0 data have allowed to improve the Run I limit of 1.6 pb in the 3-lepton search to 0.26 pb and to extend the LEP mSUGRA search [13].

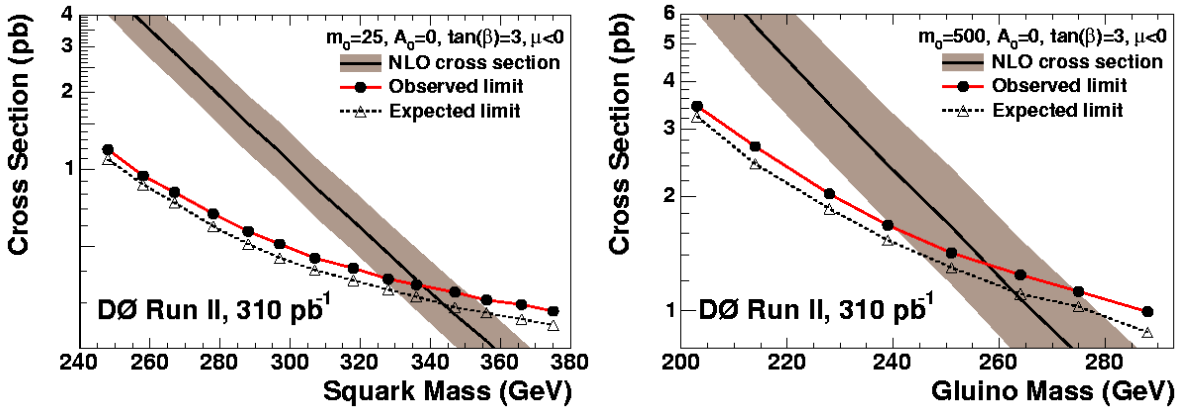

Fig. 10. D0 Run II observed limit for squark and gluino in comparison with the NLO production cross-section

11. Standard Model Higgs search

In the SM, the Higgs boson is crucial to the understanding of electroweak symmetry breaking and the mass generation of electroweak gauge bosons and fermions. However, this particle has not yet been observed. The mass of the Higgs boson is not predicted in the SM. Precision measurements in particle physics constrain the Higgs mass to $114 < m_H$ [MeV/c^2] < 260. The low mass region of 120–130 GeV/c^2 is available to a search for the Higgs at the Tevatron. Therefore, a search for the Higgs boson is one of the most important goals of the D0 experiment.

In 2003, the Tevatron Higgs sensitivity study was updated for the low Higgs mass region. The full detector simulation was used and an optimization of the analysis was done. Several searches for the SM Higgs boson have been performed using the D0 data from Run II. In particular, the Higgs boson was searched in the $p\bar{p} \to WH \to Wb\bar{b}$ [14] and $p\bar{p} \to H \to WW^{(*)}$ [15] channels. No evidence for the Higgs particle has been found. The number of events observed is consistent with the expectation from the background. Upper limits on the production cross section times the branching ratio have been derived: $\sigma(p\bar{p} \to WH) \times BR(H \to b\bar{b}) \leq 9.0$ pb and $\sigma(p\bar{p} \to H) \times BR(H \to WW^{(*)}) \leq 5.6$ pb at the 95% CL for the expected Higgs mass 115 and 120 GeV/c^2, respectively.

12. Conclusion

The D0 detector is working well with a high data taking efficiency. A number of physics results have been obtained recent years. New results in *B* and Top quark physics based on higher statistics are anticipated. New measurements in QCD and electroweak physics are planned. The SM Higgs and new phenomena physics searches are in progress.

During the D0 detector upgrade in 2006, a new silicon tracker Layer "0" was installed with improvements in *b*-tagging. The Tevatron luminosity is planned to be still further increased. The Tevatron operation and data taking at D0 and CDF will continue to 2009.

References

1. G.D. Alkhazov, V.L. Golovtsov, V.T. Kim, A.A. Lobodenko, P.V. Neustroev, G.Z. Obrant, Yu.A. Scheglov, N.K. Terentyev, L.N. Uvarov, S. L. Uvarov and A.A. Vorobyov, in *PNPI-XXV, High Energy Physics Division. Main Scientific Activities 1997–2001*, Gatchina, 2002, p. 124.
2. V.M. Abazov *et al*., Nucl. Instr. Meth. A **565**, 463 (2006).
3. V.M. Abazov *et al*., Nucl. Instr. Meth. A **552**, 372 (2005).
4. V.M. Abazov *et al*., Phys. Lett. B **626**, 35, 45, 55 (2005); Phys. Rev. D **74**, 112004 (2006).
5. CDF and D0 Collaborations and Tevatron Electro-Weak Working Group, hep-ex/0603039 (2006).
6. V.M. Abazov *et al*., Phys. Lett. B **622**, 265 (2005).
7. V.M. Abazov *et al.*, Phys. Rev. Lett. **93**, 162002 (2004) ; **94**, 221801 (2005); V.M. Abazov *et al*., Phys. Lett. B **639**, 151 (2006).
8. V.M. Abazov *et al.*, Phys. Rev. Lett. **94**, 151801, 152002, 161801 (2005) ; **95**, 051802, 141802 (2005); V.M. Abazov *et al.*, Phys. Rev. D **71**, 072004 (2005); Phys. Rev. D **71**, 091108(R) (2005).
9 V.M. Abazov *et al*., Phys. Rev. Lett. **94**, 042001, 102001, 182001, 232001 (2005), **97**, 241801 (2006); V.M. Abazov *et al*., Phys. Rev. D **74**, 031107(R) (2006).
10. V.M. Abazov *et al*., Phys. Rev. Lett. **94**, 071802 (2005).
11. V.M. Abazov *et al*., Phys. Rev. Lett. **97**, 021802 (2006).
12. V.M. Abazov *et al*., Phys. Rev. Lett. **95**, 091801, 161602 (2005).
13. V.M. Abazov *et al*., Phys. Rev. Lett. **93**, 141801 (2004) ; **94**, 041801 (2005) ; **95**, 151801, 151805 (2005); V.M. Abazov *et al*., Phys. Rev. D **71**, 071104(R) (2005).
14. V.M. Abazov *et al*., Phys. Rev. Lett. **94**, 091802 (2005).
15. V.M. Abazov *et al*., Phys. Rev. Lett. **96**, 011801 (2006).